Table 1. Gas exchange parameters under normal atmospheric conditions (330 µbar CO_2, 210 mbar O_2) and saturating light. A: net assimilation rate, D^d: dark respiration rate (both in µmol CO_2 m^{-2} s^{-1}), T: transpiration rate (mmol H_2O m^{-2} s^{-1}); n.s.: no significant change

	Control plants	Exposed plants	% relative change
A	5.0 ± 0.2	3.4 ± 0.1	−31.5
D^d	0.27 ± 0.05	0.22 ± 0.06	n.s.
T	0.96 ± 0.06	0.62 ± 0.03	−35.4

Table 2. Photosynthetic parameters calculated from gas exchange rates as a function of intracellular CO_2 partial pressure. V_m^c: maximum carboxylation velocity, A_m: maximum assimilation rate, D^l: rate of dissimilative respiration in the light (all rates in µmol m^{-2} s^{-1}), Γ: CO_2 compensation point (µbar), q_g: ratio of conductances at maximum aperture (at low CO_2) to those at minimum aperture (in the dark); n.s.: no significant change

	Control plants	Exposed plants	% relative change
V_m^c	34.7 ± 1.2	26.9 ± 0.9	−22.3
A_m	9.8 ± 0.4	9.4 ± 0.4	n.s.
D^l	0.75 ± 0.09	0.77 ± 0.05	n.s.
Γ	48.2 ± 0.9	54.0 ± 1.4	+12.0
q_g	6.3 ± 1.4	4.1 ± 0.9	n.s.

phate, is not affected by exposure to motor vehicle emissions near the highway. This runs contrary to the typical effects of stress, which usually interfere with the maximum net assimilation rate[6, 7] or impair both parameters proportionally[2, 8].

The exclusive reduction of maximum carboxylation velocity could be explained as follows:

1. The amount of ribulose-1,5-bisphosphate carboxylase (= Rubisco) might be reduced after exposure. However, this is very unlikely, as Rubisco is present in excess.
2. The activity of Rubisco might be reduced due to a Mg^{2+} deficiency resulting in a lack of enzyme activation.
3. NO_x might cause pH changes by acidifying the cytoplasm, which in turn would impair the activation of Rubisco.

The dissimilative respiration in the light D^l (i.e. the CO_2 release resulting from mitochondrial respiration, which is not identical with photorespiration), is unaffected in the exposed plants. Therefore, the decline in V_m^c results in a slight rise in the CO_2 compensation point.

The values for the regulation capacity of the stomata (q_g in table 2, i.e. the ratio of conductances at maximum aperture at low CO_2 to those at minimum aperture in the dark) show a slight decrease. This leads to the question whether, and to what extent, the net photosynthesis rates of exposed plants are limited by reduced stomatal conductances. The effects of changes in stomatal conductance and photosynthetic metabolism on the assimilation rates can be evaluated on the basis of the $A(p_i^c)$ curves by using the supply function as described by Ball and Farquhar[7] and Jones[9]. In the figure the supply functions are the broken lines which connect the points on the $A(p_i^c)$ curves corresponding to the values under normal atmospheric conditions to the point on the x-axis where p_i^c equals the ambient CO_2 partial pressure p_a^c. The slopes of these are equal to the negative of the conductance to diffusion of CO_2 under normal conditions. If the stomata had been insensitive to the exposure at the highway, the changes in photosynthetic capacity would have led to only small reductions in photosynthesis rates (intersection of the steeper supply function with the lower $A(p_i^c)$ curve). The observed rates (intersection of the flatter supply function with the lower $A(p_i^c)$ curve) are still below this value for unaffected conductance. Therefore, a co-limitation of the assimilation rates of exposed plants by both stomatal conductance and photosynthetic capacity must be assumed. For a numerical estimate, limitation factors were calculated for both treatments according to the 'differential method'[9], and resulted in 0.50 and 0.55 for control and exposed plants, respectively. The limitation of photosynthesis due to diffusive resistance thus increased by 10% in the exposed plants.

The following conclusions can be drawn:

1. Both the stomata and photosynthetic apparatus of spruce needles were affected by road site conditions near the highway.
2. The regulation capacity of the stomata was reduced.
3. The carboxylation velocity of Rubisco was affected by the road side conditions.
4. The reduction in the net photosynthesis rate under normal atmospheric conditions resulted from co-limitation by both stomatal conductance and photosynthetic metabolism.
5. In cases where only a slight impairment of the photosynthetic apparatus occurs, gas exchange measurements give more accurate information about the nature of stress effects.

Acknowledgments. This work was supported by a grant from the Bayerisches Staatsministerium für Unterricht und Kultus to Prof. B. Hock.

1 Flückiger, W., Flückiger-Keller, H., and Oertli, J.J., Experientia *34* (1978) 1274.
2 Kammerbauer, H., Selinger, H., Römmelt, R., Ziegler-Jöns, A., Knoppik, D., and Hock, B., Envir. Pollut. (A) *42* (1986) 133.
3 Keller, Th., Forstwiss. ZentBl. *104* (1985) 312.
4 Farquhar, G.D., and von Caemmerer, S., in: Encyclopedia of Plant Physiology, N.S., vol. 12B, p. 549. Springer-Verlag, Berlin 1982.
5 Selinger, H., Knoppik, D., and Ziegler-Jöns, A., Progress in Photosynthesis Research, vol. 4, pp. 299–232. Ed. J. Biggins. 1987.
6 Von Caemmerer, S., and Farquhar, G.D., Planta *160* (1984) 320.
7 Ball, M.C., and Farquhar, G.D., Pl. Physiol. *74* (1984) 7.
8 Selinger, H., Knoppik, D., and Ziegler-Jöns, A., Forstwiss. ZentBl. *105* (1986) 239.
9 Jones, H.G., Plant Cell Envir. *8* (1985) 95.

0014-4754/87/101124-02$1.50 + 0.20/0

A new semisynthetic ergot peptide alkaloid: DCN 203-922

R.K.A. Giger[1], H.R. Loosli, M.D. Walkinshaw, B.J. Clark and J.M. Vigouret

Preclinical Research, Sandoz Ltd., CH-4002 Basel (Switzerland), 28 April 1987

Summary. We report the synthesis, stereochemistry and preliminary pharmacological evaluation of DCN 203-922, a novel ergot alkaloid of the cyclol type, which contains in its peptide moiety the uncommon amino acid L-allo-isoleucine.
Key words. DCN 203-922; DH-β-ergokryptine; ergot peptide alkaloid.

Over several decades ergot peptide alkaloids have found broad application in medicine[2, 3] and have stimulated continuous interest in pharmacology because of their unique ability to interact directly with various neurotransmitter systems in the periphery as well as in the CNS.

The cyclic peptide moiety controls their unusual pharmacokinetics and also provides the main site for metabolic attack. There is a substantial effect in the liver first pass, where degradation of the proline ring gives rise to a large amount of the 8′-hydroxymetabolite. However, this metabolite usually

shows a profile of action in vitro similar to the corresponding parent compound[4] contributing to the activity of these drugs. This metabolic pathway, therefore, is a desirable property since it ensures that the profile of action of the compound does not change with time as a result of metabolism.

Results of a systematic variation of the peptide moiety, accumulated in our company during the last decade, indicate that any stereochemical modification of the skeleton of the cyclol portion considerably diminishes the affinity to most of the monoaminergic binding sites and also dramatically reduces the pharmacodynamic effects of these compounds.

Dihydro-β-ergokryptine (**I**, DHBE) attracted our attention, as it is the only ergot peptide alkaloid, which has an additional asymmetric center (C-13′) on a side chain attached at the tricyclic skeleton at the carbon atom C-5′, which is itself asymmetric.

The contiguous arrangement of the asymmetric carbon atoms C-5′ and C-13′ therefore raises interesting questions about the possible conformational freedom and the preferred conformation of the sec.-butyl side chain of DHBE.

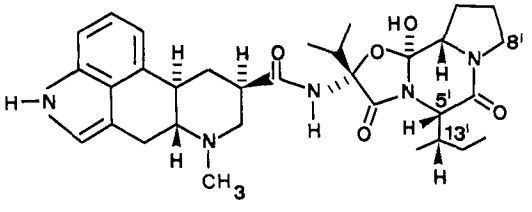

I

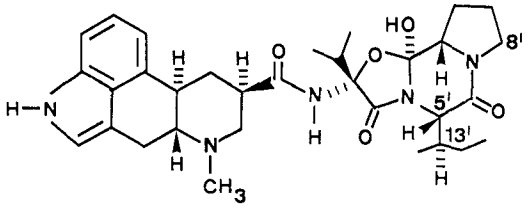

II

The objective of this work was to investigate this matter by comparing the properties of DHBE and its epimer (**II**), in which only the configuration on the sec.-butyl side chain is inverted.

Whereas DHBE contains as a building block the commonly-occurring amino acid *L-iso-leucine* (L-Ile) (**III**), the so far unknown diastereomer (**II**) with R-configuration at C-13′ incorporates in its peptide moiety L-allo-isoleucine (L-aIle) (**IV**), an amino acid which is rare in nature[5], though it is found in individuals suffering from a particular metabolic disease[6].

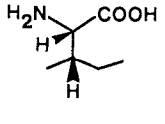

III

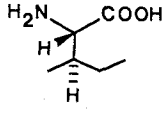

IV

Synthesis. The new compound (**II**) was prepared using the know-how earlier developed for the total synthesis of ergotamine[7] following the synthetic scheme described in figure 1. The major difficulty encountered in this synthesis was the availability of L-aIle (**IV**), which at that time was available from a commercial source only in very limited amounts.

After peptide formation with N-protected L-proline, the dipeptide (**V**) is hydrogenated and cyclised to the L-allo-isoleucyl-L-proline lactame (**VI**). Subsequent reaction with S-(+)-benzyloxyisopropyl malonic acid gives the monoethylesterchloride of the cyclol acid (**VII**). Via the azide a modified Curtius degradation leads, after hydrogenation of (**VIII**), to the L-allo-isoleucine-isopropylaminocyclol monohydroxychloride (**IX**). Finally dihydroxylysergic acid is activated using oxalylchloride and reacted with the aminocyclol monohydrochloride to form the desired epimer (**II**)[8], 9,10-alpha-dihydro-12′-hydroxy-2′-isopropyl-5′alpha-(R-1-methylpropyl)-ergotaman-3′,6′,18-trione, which was given the code number 203-922.

The problem concerning the synthesis of L-aIle (**IV**) was later circumvented using optically-active (−)-R-3-methylvaleric acid (**X**) as starting material, which is prepared as described in the literature[9] (fig. 2). Subsequent bromination of (**X**) gives as expected a diastereomeric mixture of the bromo derivatives (**XI**), which after formation of the acid chlorides and condensation with L-prolinemethylester (**XII**) leads to the corresponding diastereomeric bromo derivatives (**XIII**).

After substitution of the bromine atoms by the azide groups to give (**XIV**), followed by hydrogenation, a 1:1 mixture of the diastereomeric diketo-piperazines (**VI**) and (**VIa**) is obtained. Easy separation by chromatography gives the desired key intermediate L-proline-L-aIle-lactame (**VI**), already employed as an intermediate in the synthesis described above (fig. 1). This synthetic sequence allows the preparation of larger amounts of 203-922.

In the meantime, two new approaches for the synthesis of L-aIle have been published[10,11].

Results and discussion. 203-922 was obtained by crystallization from ethylacetate-ether, m.p. 190-1 °C; $[\alpha]_D^{20} = -43.5°$; (c = 0.5 in pyridine), MW 577,72, C32H43N5O5. The physico-chemical data indicate that 203-922 can be clearly distinguished from DHBE in many ways, for instance, on the basis of ^{13}C-NMR data which show that the chemical shifts of the isoleucine carbon atoms C-14′ and C-16′ are significantly different (table 1), as a consequence of the inversion of the isoleucine carbon atom 13′.

Table 1. ^{13}C-NMR measurements. All other signals differ by less than 0.5 ppm.

Atom	DHBE	203-922	Delta [ppm]
5′	61.0	61.6	−0.6
6′	167.1	167.5	−0.4
13′	40.4	40.6	−0.2
14′	28.6	27.4	+1.2
15′	13.4	13.3	+0.1
16′	16.4	17.5	−1.1

Molecular shape: Conformation and X-ray structure. Crystals of both DHBE and 203-922 were grown from pure ethanol solution for the purpose of comparison. They were found to be quite different morphologically, with DHBE growing as well-formed prisms and 203-922 forming thick columnar needles (fig. 3).

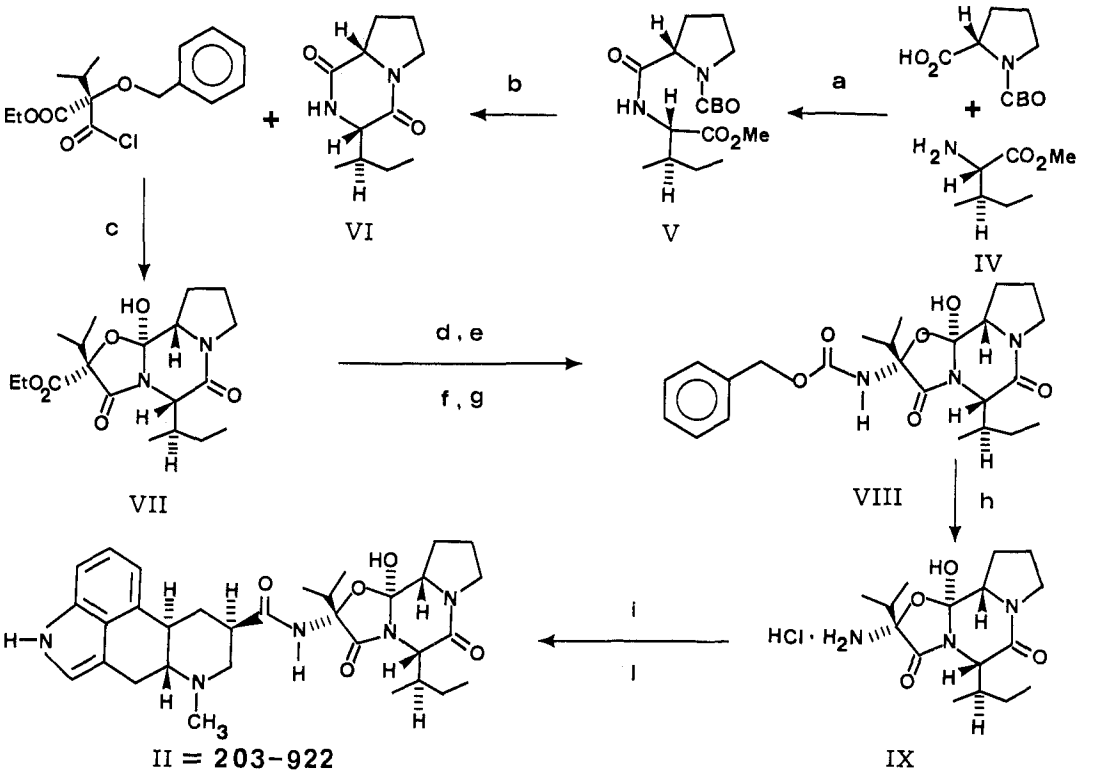

Figure 1. a: COIm2,THF 93%; b: H2,Pd-C,To 60%; c: H2,Pd-C 78%; d: NaOH 91%; e: PCl5 and f: NaN3 66%; g: BzOH 92%; h: H2, Pd-C 76%; i: (CF3CO)2,CF3COOH, and l: DHLS 70%.

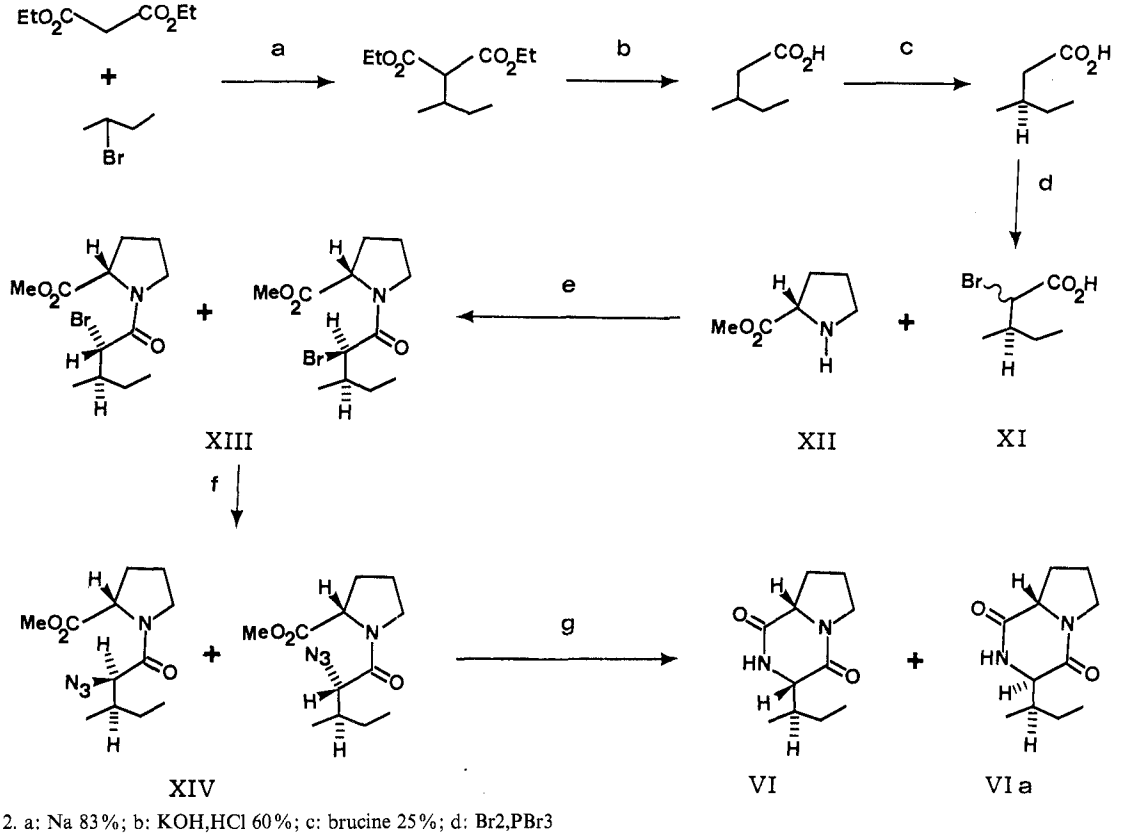

Figure 2. a: Na 83%; b: KOH,HCl 60%; c: brucine 25%; d: Br2,PBr3 55%; e: n-PrPOCl2,DMF,CHCl3; 98% f: NaN3,DMSO 94% and g: H2,Pd-C 90%.

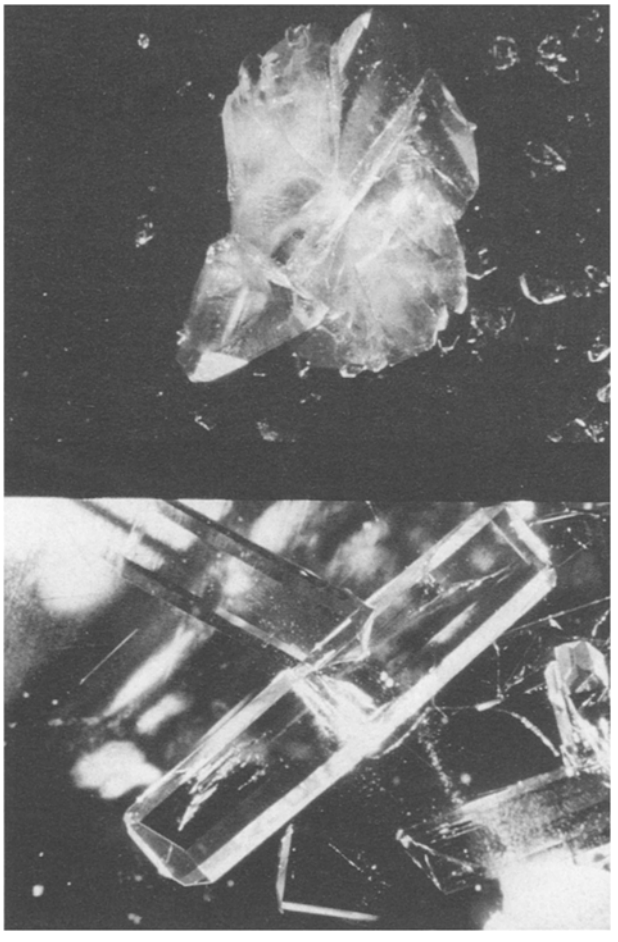

There were also significant differences in solubility (at pH < 2 DHBE is 10 times more soluble than 203-922, whereas at pH > 4 DHBE is less soluble than 203-922 in hydrochloric acid) and melting point (DHBE=189 °C, 203-922=169 °C). It was most surprising, therefore, to find that both compounds crystallize in space group P21 with nearly isomorphous unit cells:

DHBE a = 12.226(4),b = 18.181(10),c = 15.681(9) Å,
β = 104.34(4)°
203-922 a = 12.307(4),b = 18.279(3),c = 15.553(6) Å,
β = 106.05(3)°

Details of the full crystallographic analysis will be published later. In both unit cells, there are two crystallographically independent molecules, drawings of which are given in figure 4. The two molecules within each structure show significant conformational differences. Despite the presence of the important C(18)-0...C(12′)-0 intramolecular hydrogen bond in both molecules, the Φ and Ψ angles of the peptide link (table 2) differ by up to 10° with 203-922.

Table 2.

	203-922 1	203-922 2	DHBE 1	DHBE 2
Ψ C7-C8-C18-N20	139.7	150.3	142.9	142.3
Φ C18-N20-C2′-C3′	−53.6	−64.4	−54.4	−59.9
X N4′-C5′-C14′-C15′	−155.9	34.2	83.4	83.8

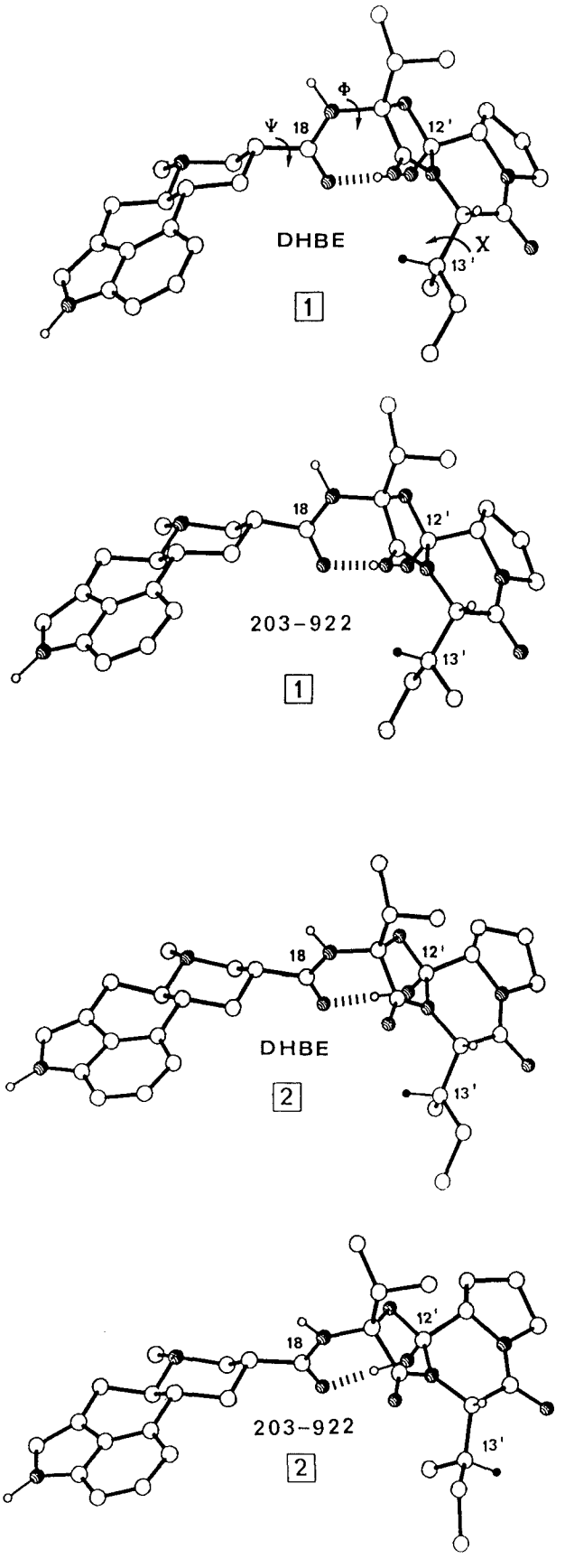

Figure 4. DHBE and 203-922: The two pairs of independent molecules.

The proline ring adopts two different envelope conformations in the two molecules. These conformational differences are found in both crystal structures, and are a consequence of the similar intermolecular hydrogen bonding and van der Waals interactions. This near isomorphism breaks down, however, in the region of the isoleucine side chain. In the DHBE structure, the L-Ile chains of the two molecules adopt identical conformations (X=83.4° and 83.8°). In the 203-922 structure, the L-aIle side chain adopts two distinct conformations (X=−155.9° and 34.2°) which do not disturb the overall crystal packing and indeed seem not to greatly affect the molecular conformation.

It is interesting to note that, depending on its conformation, the Ile chain can be within van der Waals contact with each of the four carbonyl/hydroxyl oxygens of the tricyclic peptide skeleton. Both DHBE molecules and one molecule of 203-922 (with X=34.2°) show similar interaction between the side chain and the oxygen. The alternative conformation (X=−155.9°) of the second 203-922 molecule provides a better contact with both C(18)-0 and C(12')-0 which could act in solution as a better hydrophobic shield, thus helping to preserve the intramolecular C(18)-0...C(12')-0 hydrogen bond. Molecular mechanics calculations[12] show that energies of the various staggered conformations of the L-Ile and L-aIle side chains (X=60,−60,180) differ by up to 8 kJ/mol. The X-ray structures, however, provide experimental evidence that the aIle side chain is conformationally more flexible and therefore can help to screen the intramolecular hydrogen bond more effectively. We regard this as a possible explanation of the different properties of DHBE and DCN 203-922.

Biological activity of 203-922. 203-922 and DHBE both have affinity to a variety of monoamine binding sites in brain tissue. Functionally, this results in behavioral stimulation in animals with surgical or drug-induced defects in aminergic neurotransmission, or when placed in an anxiogenic environment. Despite their structural similarity, the relative affinities of the two compounds to monoamine binding sites are different. They vary also in potency, especially by the oral route; 203-922 is, for example, about three times more effective than DHBE in reducing the duration of paradoxical (REM) sleep and increasing the duration of wakefulness[13] (table 3).

Table 3. Sleep-wakefulness cycle in the rat (n=6)

	mg/kg p.o.	Wakefulness (in % of control)	REM-sleep
203-922	10	+70	−64
DHBE	10	+ 4	−12
	30	+60	−78

The activity profile of 203-922 in the central nervous system differs from that of cerebral activators such as amphetamine and bromocriptine, in that the compound is devoid of any major effect on motor systems.

203-922 and bromocriptine both stimulate dopamine receptors, the two compounds being equiactive in inhibiting lactation in rats[14] (table 4).

Table 4. Inhibition of lactation in the rat (n=6)

	ID_{50} (mg/kg/day p.o. for 3 days)
203-922	15
Bromocriptine	12.6

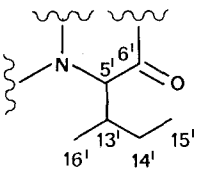

Bromocriptine

In contrast to bromocriptine, however, 203-922 does not induce behavioral excitation, and possesses central serotoninergic activity, i.e., it reduces the frequency of reserpine-induced electrical potentials in the ponto-geniculo-occipital (PGO) regions in the cat (table 5).

Table 5. Effects on reserpine-induced effects in the cat (n=6)

	Inhibition of PGO-spikes ID_{50} (mg/kg i.v.)	Behavioral depression
203-922	0.11	Reduced
Bromocriptine	> 1	Reversed (excitation)

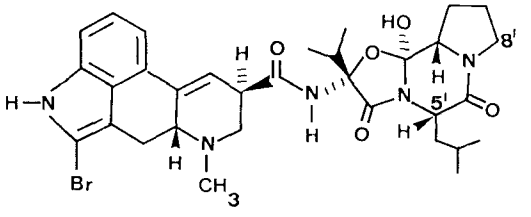

The dopaminergic activity of 203-922 is reflected also in its effects in the periphery. The compound is one of the most potent prejunctional dopamine (DA2) receptor stimulants so far described; heart rate increases in response to cardiac nerve stimulation in cats are inhibited dose-dependently from a dose of 0.5 µg/kg i.v., and this effect is prevented by pretreatment with sulpiride. Inhibition of noradrenaline efflux from sympathetic neurones mediated by prejunctional dopamine receptor stimulation appears to be the major mechanism responsible for the reductions in heart rate, blood pressure, and total peripheral resistance which it produces in hypertensive and normotensive animals, since all these effects are markedly attenuated or abolished by DA2 receptor blockade. 203-922 also inhibits renin secretion and increases sodium excretion in rats[15]; these additional actions may contribute to its antihypertensive activity.

The effects exerted by 203-922 on the central nervous system suggest that it might benefit patients (particularly the elderly) who have cognitive and affective deficits which threaten their independence and necessitate drug therapy[16]. The cardiovascular and renal effects of 203-922 are novel, and could represent a new approach to the treatment of hypertension and congestive cardiac failure.

Acknowledgment. The expert technical assistance of Mr W. Nussbaum for synthetic work is gratefully acknowledged. We also thank Ms R. Dammert for preparation of the manuscript.

1 To whom reprint requests should be addressed. Part of this paper was reported by this author at the Herbstversammlung der Schweizerischen Chemischen Gesellschaft, Bern, in October 1986.
2 Berde, B., and Schild, H.O., Ergot Alkaloids and Related Compounds. Springer, Berlin 1978.
3 Stadler, P.A., and Giger, R.K.A., Ergot Alkaloids and Their Derivatives in Medicinal Chemistry and Therapy. Alfred Benzon Symposium 20, pp. 463–85. Munksgaard, Copenhagen 1984.
4 Maurer, G., Schreier, E., Delaborde, S., Loosli, H.R., Nufer, R. and Shukla, A.P. Eur. J. Drug Metab. Pharmacokin. *7* (1982) 281 and Maurer, G., Schreier, E., Delaborde, S., Nufer, R. and Shukla, A.P., Eur. J. Drug. Metab. Pharmacokin. *8* (1983) 51.
5 Bada, J.L., Zhao, M., Steinberg, S., and Ruth, E., Nature *319* (1986) 314–316.
6 Halpern, B., and Pollock, G.E., Biochem. Med. *4* (1970) 352.
7 Hofmann, A., Frey, A.J., and Ott, H., Experientia *17* (1961) 206.
8 Giger, R.K.A., Offenlegungsschrift DE 33 03 616 A1 (1983).
9 Organic Syntheses, Coll. Vol. I 36–38 and III 495–498.
10 Bartlett, P.A., Tanzella, D.J., and Barstow, J.F., Tetrahedron Lett. *23* (1982) 619.
11 Oppolzer, W., Pedrosa, R., and Moretti, R., Tetrahedron Lett. *27* (1986) 831.
12 Lindner, H.J., Tetrahedron *30* (1974) 1127.
13 Vigouret, J.M., Buerki, H.R., Jaton, A.L., and Loew, D.M., Pharmacology *16* (1978) 156.
14 Shelesnyak, M.C., Proc. 1st int. Congr. Endocr., p. 677. Copenhagen 1960.
15 Siegl, H., unpublished results.
16 Giger, R.K.A., and Vigouret, J.M., International Congress of Gerontology. New York, July 1984.

0014-4754/87/101125-06$1.50 + 0.20/0